Structure, Volume *23*

Supplemental Information

Charge-Triggered Membrane Insertion of Matrix Metalloproteinase-7, Supporter of Innate Immunity and Tumors

Stephen H. Prior, Yan G. Fulcher, Rama K. Koppisetti, Alexander Jurkevich, and Steven R. Van Doren

Supplemental Information

Charge-Triggered Membrane Insertion of Matrix Metalloproteinase-7, Supporter of Innate Immunity and Tumors

Stephen H. Prior, Yan. G. Fulcher, Rama K. Koppisetti, Alexander Jurkevich[1], and Steven R. Van Doren*

Biochemistry Department, University of Missouri, 117 Schweitzer Hall, Columbia, MO 65211, USA

[1] Molecular Cytology Core, 120 Bond Life Sciences Center, University of Missouri, Columbia, MO 65211, USA

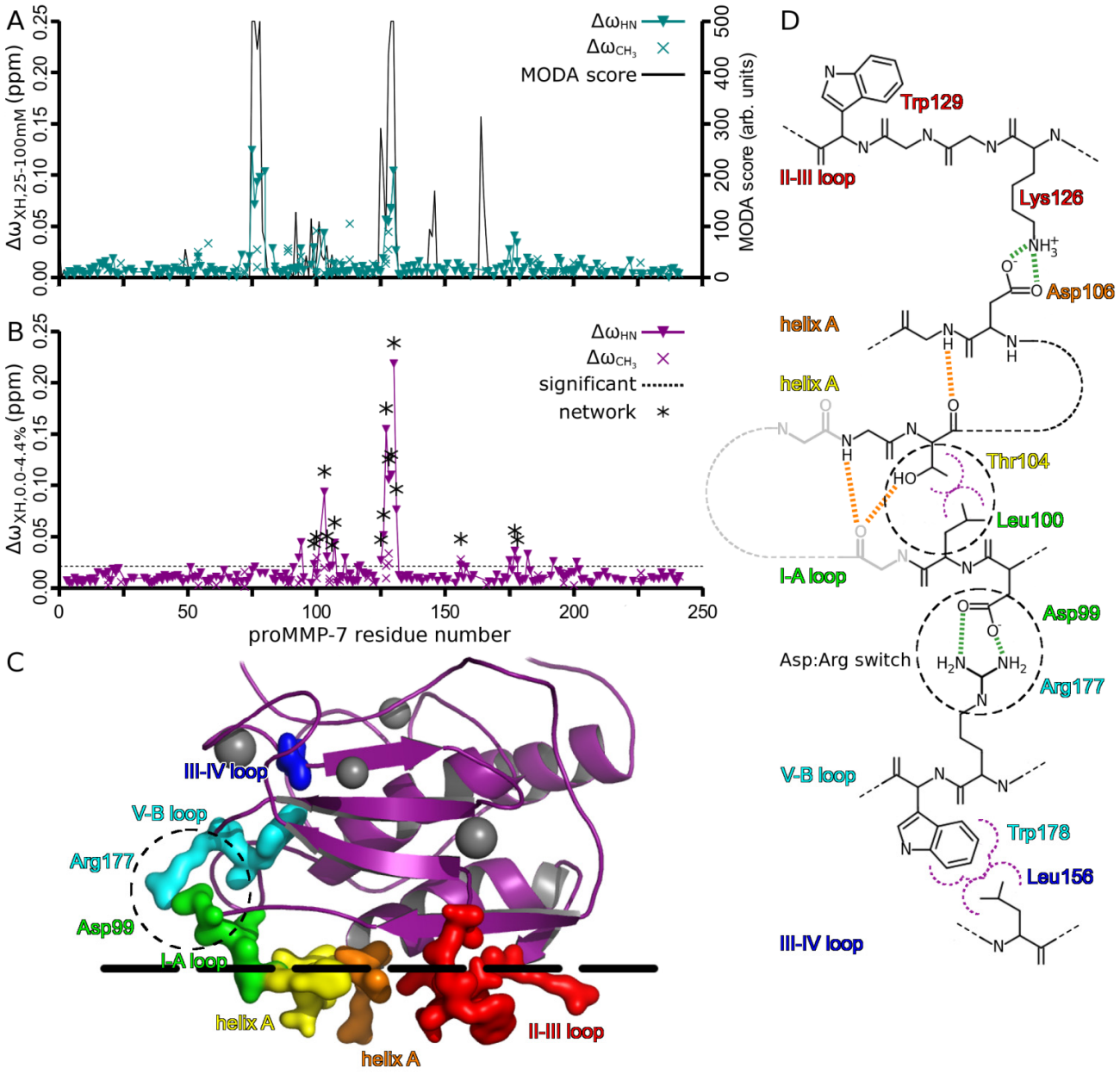

Figure S1, related to Figure 1. NMR peak perturbations suggest interfaces for bicelles, a bicelle-triggered pathway that could convey allostery, and agreement with structure-based prediction of zwitterionic membrane binding. A) Zwitterionic DMPC/DH^{6}PC bicelle-induced NMR peak shifts (*cyan*) of proMMP-7(E195A) are in good agreement with the MODA predictions of membrane binding (*black line*). B-D) Evidence of potential allosteric transmission switched into structural connectivity by bicelles. B) CSPs induced by ~6 CS per bicelle (*purple*) are plotted. C) Sites of CS-induced CSPs plotted on the structure (PDB: 2mzi) form a continuous arc (*colored sticks*). The arc begins at the II-III loop (*red sticks*) and traverses the N-terminal end of helix A (*orange* and *yellow sticks*), before crossing from the I-A loop to the V-B loop (*green* and *cyan* sticks, respectively) and terminates in the active site just prior to strand IV (*blue sticks*). For clarity, the pro-domain and discontinuous CSPs have been omitted from C). Residues highlighted in C) are represented in B) by *asterisks*. Approximate location of lipid phosphate groups is shown as *black dashed line*. D) Schematic representation of proposed allosteric switching**.** Communication between helix A and loop V-B may proceed via two changes: Bicelles induce salt bridging between Asp99 and Arg177 (*lower dashed circle*). CS-doped bicelles disrupt hydrophobic contacts between Thr104 and Leu100 (*upper dashed circle*) while the Thr104 hydroxyl group then donates an H-bond to Pro101. Leu156 contacts Arg66 of the autoinhibitory salt bridge. Colors match panel C). Salt bridges are shown as *green dashes,* H-bonds as *orange dashes,* and hydrophobic contacts as *purple arcs.*

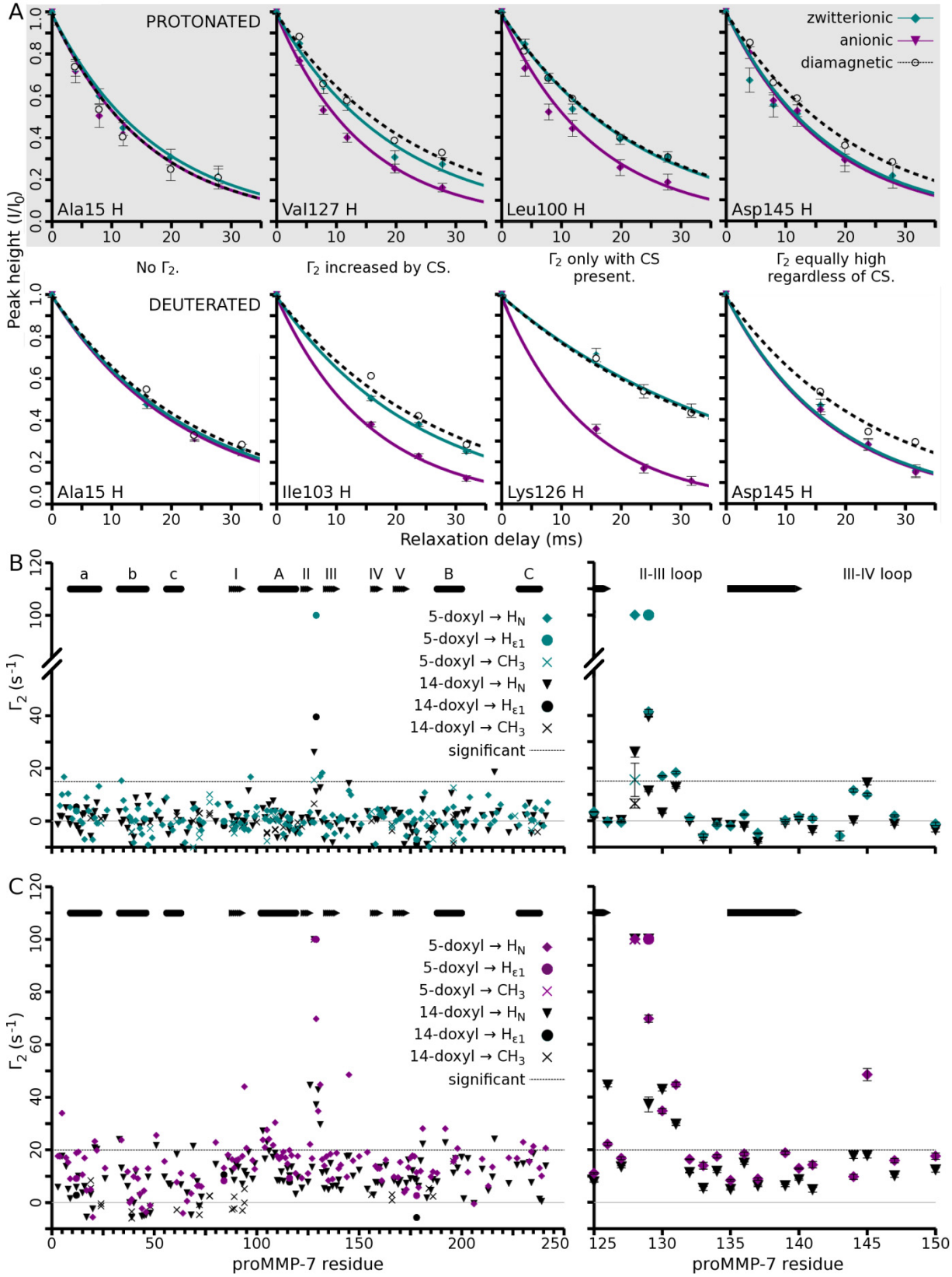

Figure S2, related to Figure 2. Proximity of bicelles to proMMP-7 revealed by NMR PREs from spin-labeled DPPC. DMPC/ DH^6PC bicelles (1:2; q=0.5; 150 mM total lipid) were used when zwitterionic (*cyan*) or made anionic by CS at ~3/ leaflet (*magenta*). 5- or 14-doxyl DPPC was doped in to ~1/ bicelle. (A) Examples of exponential decays with the length of the PROJECT-CPMG pulse train (which suppresses $^3J_{HH}$ couplings) in the following states of the bicelles: diamagnetic without doping (dashed lines), paramagnetic from 14-doxyl DPPC doping of zwitterionic bicelles (*cyan*), and bicelles harboring both CS (anionic) and paramagnetic 14-doxyl DPPC (*magenta*). The top row of panels

were measured on bicelle complexes with protonated zymogen ($^{1}H/^{15}N$; gray background) while the second row were measured on bicelle complexes with deuterated zymogen ($^{2}H/^{15}N/^{13}CH_3$ of ILV). Ala15 in the pro-domain is an example lacking PRE. Leu100, Ile103, Lys126, and Val127 are sites that report CS-increased proximity to the bicelles. Asp145 is a location moderately close to bicelles but insensitive to their charge and to the orientation of binding. Error bars represent one σ of the spectral noise. (B, C) Plots of PREs (Γ_2) per residue of proMMP-7 from spin-labeled bicelles lacking (B) or containing CS (C). *Diamonds* indicate the PRE on the amide proton by the shallow 5-doxyl spin label. *Circles* represent the PRE on Trp ε_1 protons. *Triangles* represent the PRE on the amide proton from the deep 14-doxyl spin label. *Crosses* represent methyl protons. The *dotted line* represents the smallest Γ_2 value deemed significant, i.e. 15 s^{-1} for the zwitterionic bicelles and 20 s^{-1} for the anionic bicelles. Errors are propagated from uncertainties in peak heights using standard rules. In (C), PREs in the pro-domain are suggestive of lightly populated close approaches of the pro-domain to bicelles that are distinct from the predominant mode of bicelle binding to the distal side of the catalytic domain. Consistent with CS recruiting fleeting encounters with the pro-domain, CS also mildly increases fluorescence emission from the IANBD fluor conjugated to S56C in the pro-domain (Fig. 4B).

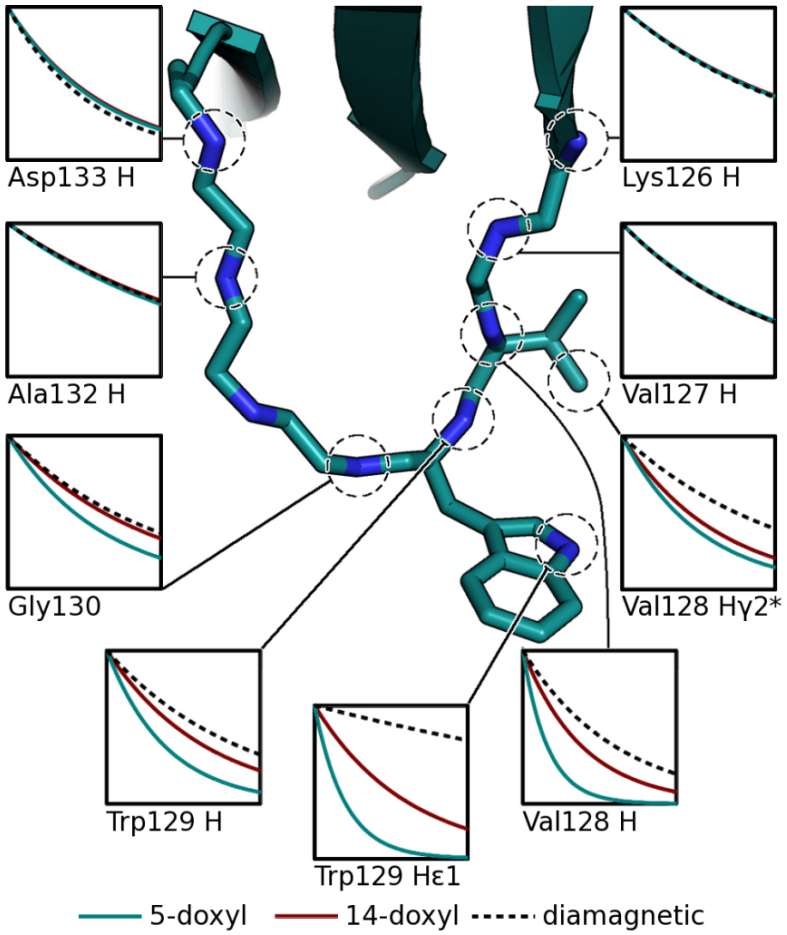

Figure S3, related to Figure 2. The sensitivity of the nadir (or tip) of the II-III loop to paramagnetic relaxation by nitroxide-doped zwitterionic bicelles implies close proximity. The dashed lines indicate the control diamagnetic ^{1}H NMR relaxation with zwitterionic DMPC/DH^{6}PC (1:2) bicelles. The red curves depict the ^{1}H relaxation enhanced by paramagnetic doping with 14-doxyl DPPC (~1/leaflet) placing the nitroxide group deep in the interior of the DMPC bilayer phase of the bicelles. The cyan curves depict the ^{1}H relaxation enhanced by the paramagnetic doping with 5-doxyl DPPC with the nitroxide at a shallow level in the DMPC bilayer phase.

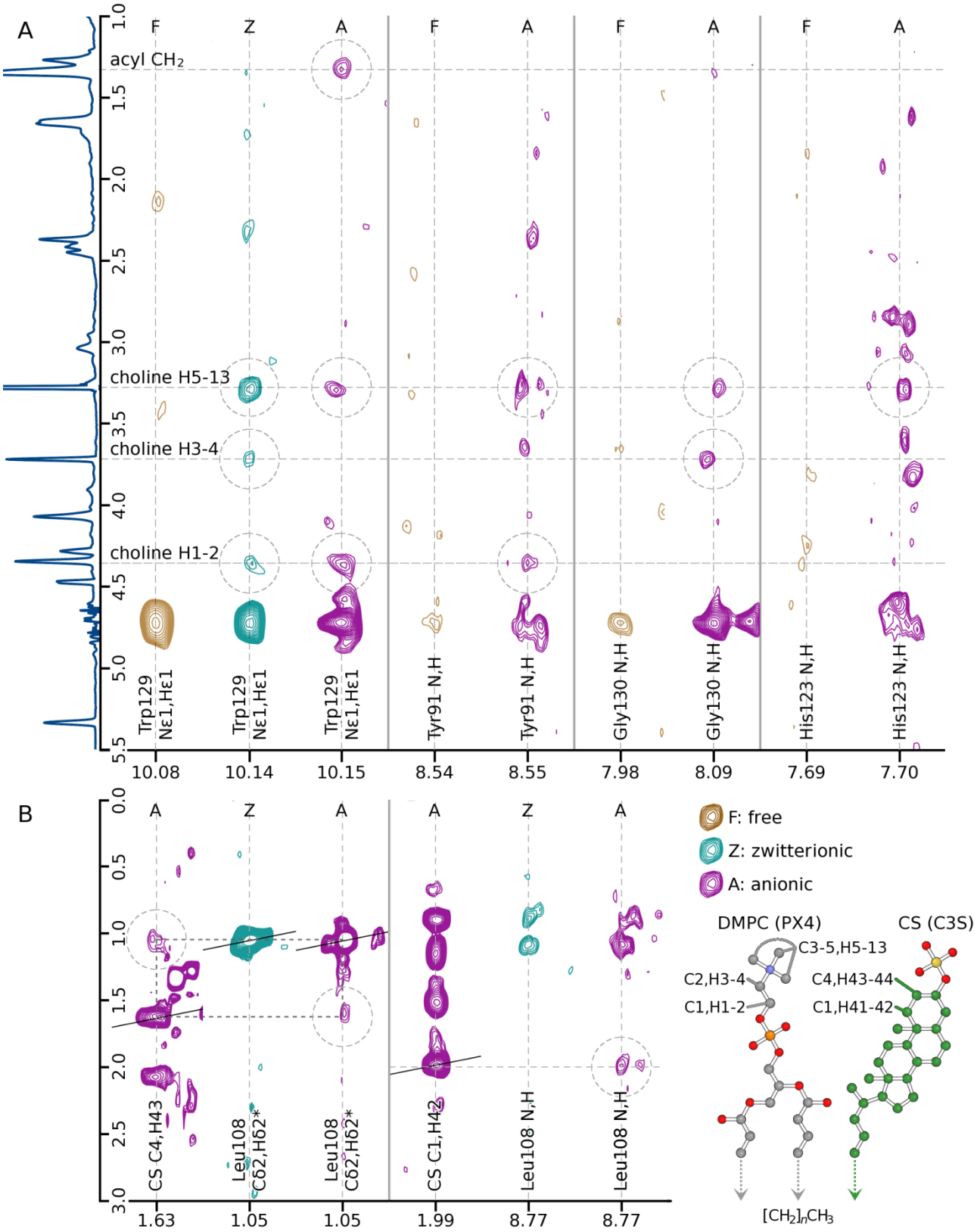

Figure S4, related to Figure 2. NOEs from phosphatidylcholine and cholesterol sulfate components of bicelles to proMMP-7(E195A). (A and B) Amide groups participating in the NOESY strips are noted. The strips at left in (B) involve the aliphatic groups of CS and Leu108 listed. NOESY strips with the zwitterionic bicelles are cyan and with cholesterol sulfate-containing bicelles are magenta. Plots for the free state of proMMP-7 use gold contours. Groups from DMPC and CS assigned unambiguously to NOEs with proMMP-7 are pointed out at right in (B).

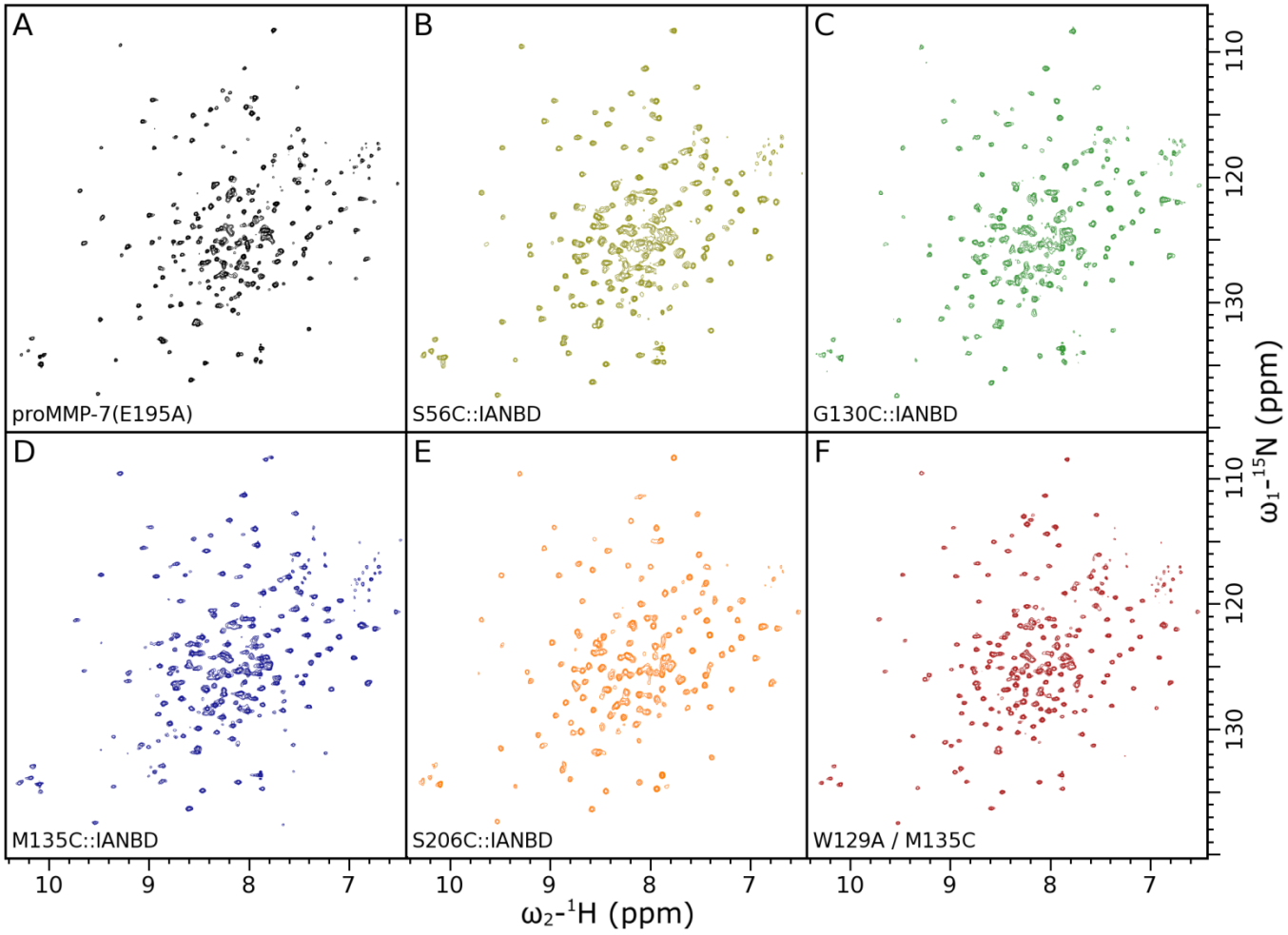

Figure S5, related to Figure 4. Single Cys and IANBD substitutions at surface positions used in this study preserve the ^{15}N TROSY spectrum characteristic of proMMP-7(E195A), implying preservation of the overall structure.

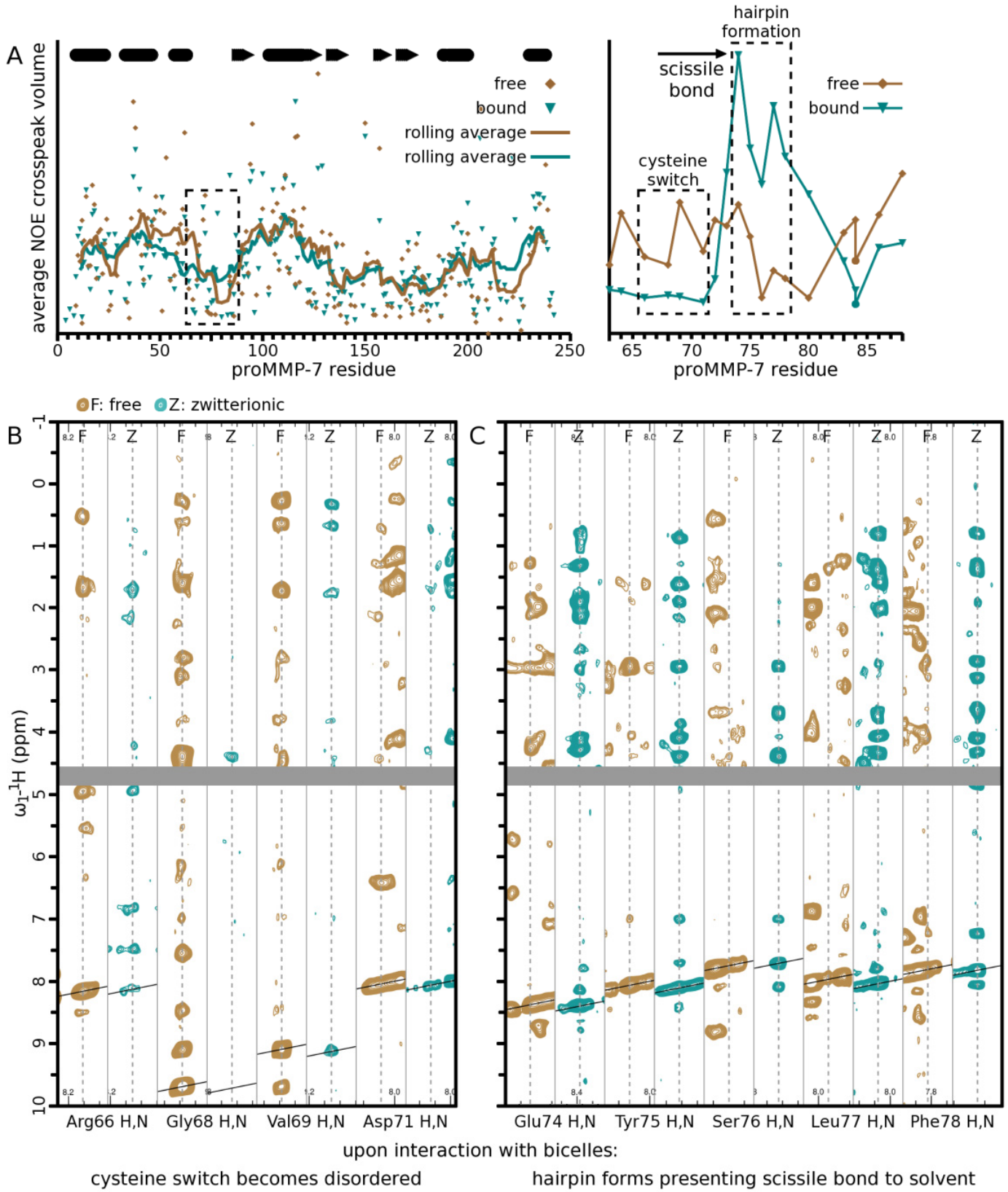

Figure S6, related to Figure 6**.** Allosteric structural changes priming auto-inhibitory and scissile linker regions for activation by interaction with bicelles. A) Increased NOE cross peak volumes are associated with structurally defined regions. *Gold diamonds* represent average NOE cross peak volumes obtained from methyl-labeled proMMP-7 free in solution; *cyan triangles* represent the normalized cross peak volumes obtained from methyl-labelled proMMP-7 interacting with 0.5 mM bicelles; *lines* represent 11-point rolling averages. Maximal NOE volumes are observed in helical regions, and lowest volumes occur in long disordered loops, particularly the proteolytically vulnerable

linker and S_1' specificity loops. The area in the *dashed rectangle* is expanded in the panel at right to better show the changes that occur in the scissile linker region upon interaction with bicelles: The Cys switch region moves from NOE volumes characteristic of minimal order to volumes characteristic of no order. This corresponds to the observed loss of the Arg66-Asp71 salt bridge. The dramatic increase in NOE volumes in the area around the scissile bond suggests an increase in order there from formation of a hairpin centered on the scissile bond and presenting it to the solvent. The cross peak volumes in the inset are derived from a protonated sample. B) NOE strips corresponding to the Cys switch region. NOE cross peaks of the free form (*gold*) are far more voluminous than their counterparts in the presence of bicelles (*cyan*). The region corresponds to the first *dashed box* of the inset of panel A. (C) NOE strips corresponding to the flexible, scissile linker region corresponds to the second *dashed rectangle* in the expansion at right in A.

Table S1, related to Figure 1. Translational diffusion coefficients of bicelles.[¶]

Lipid composition	**D_s (10^{-10} m^2/s) on 800 MHz**	**D_s (10^{-10} m^2/s) on 600 MHz**	**Mean D_s (10^{-10} m^2/s)**
50 mM DMPC, 100 mM DH^6PC	1.016	1.036	1.026 ± 0.014 [†]
50 mM DMPC, 100 mM DH^6PC, 1.11 mM cholesterol sulfate	1.004	1.029	1.016 ± 0.017 [†]

[¶] Measured from methyl multiplet of DMPC using an NMR pulse sequence encoding longitudinal eddy current decay with bipolar pulse pairs (LED-BPP) (Wu et al., 1995).

[†] The mean ± SD of measurements at 600 and 800 MHz.

Table S2, related to Table 2 and Figure 2. Frequent, apparent contacts between DMPC bilayer and proMMP-7.

Consistent contacts in ensemble	**2mzh**: DMPC/DH^{6}PC, zwitterionic		**2mzi**: CS + DMPC/DH^{6}PC, anionic	
H-bonds[¶]				
			Arg92 Hη2	PX4* O8
			Arg92 Hη2	PX4 O2[†]
			Tyr96 Hη	C3S O2[‡]
			Arg107 Hε	PX4 O8
			Asn114 Hδ2	PX4 O1
			Phe124 H	PX4 O1
			Arg125 Hη2	PX4 O1
			Arg125 Hη2	PX4 O8
			Lys126 Hζ	PX4 O6
			Trp129 Hε1	PX4 O3†,O1,or O4†
Salt bridges[¶]				
	Arg98 Nη1	PX4* O1†	Lys87 Nζ	PX4 O8
	Arg98 Nη1	PX4 O3†	Arg92 Nη2	PX4 O2
	Arg98 Nη2	PX4 O1	Arg92 Nη2	PX4 O8
	Arg140 Nη1	PX4 O2†	Arg107 Nη2	PX4 O8
	Arg140 Nη1	PX4 O3	Arg125 Nη2	PX4 O1
			Arg125 Nη2	PX4 O8
			Lys126 Nζ	PX4 O6
Hydrophobic[‖]				
	Trp129 pyrrole	PX4 C1-C5[§]	His102 imidazole	PX4 C1-C5[§]
	Trp129 phenyl	PX4 C1-C5	Ile103 butyl	PX4 C24-C27[&]
			Ile103 butyl	PX4 C31-C33
			Arg107 C_ali	PX4 C24-C27
			Arg107 C_ali	PX4 C20-C22
			Lys111 C_ali	PX4 C1-C5
			Lys111 C_ali	PX4 C6-C8
			His123 C_ali	PX4 C1-C5
			Lys126 C_ali	PX4 C28-C30
			Lys126 C_ali	PX4 C31-C33
			Val127 butyl	PX4 C1-C5
			Val128 butyl	PX4 C24-C27
			Val128 butyl	PX4 C34-C36
			Trp129 pyrrole	PX4 C10-C13[&]
			Trp129 phenyl	PX4 C34-C36
			Trp129 C_ali	PX4 C24-C27

[¶] observed in > 75% of members of ensemble
* PX4 is Protein Data Bank naming of DMPC.
[†] Phosphate oxygen
[‡] Sulfate oxygen
[‖] Among the groups of atoms listed, an average of at least two hydrophobic contacts per member of the ensemble are observed.
[§] Choline head group, numbered by increasing distance from phosphate
[&] Carbons of the fatty acyl chain esterified at the 1-position are numbered C23-C36 with increasing distance from the ester. Carbons of the acyl chain esterified at the 2-position are numbered C9-C22.

Movie S1, related to Figures 3A and 2A. Simulated trajectory of diffusion of proMMP-7 on the zwitterionic DMPC bilayer. The molecular dynamics were restrained by the NMR-measured, PRE-based distances between the proenzyme and zwitterionic bicelles (and by NOEs within proMMP-7). One sphere is used to represent the catalytic domain and another sphere for the pro-domain. The axes plotted are the coordinate system defined in Figure 2. The grid marks the average plane of the phosphoryl moieties of the head groups.

Movie S2, related to Figures 3B and 2B. Simulated trajectory of diffusion of proMMP-7 on the DMPC bilayer made anionic by cholesterol sulfate added. The molecular dynamics were restrained by numerous distances based on PREs and NOEs between the proenzyme and cholesterol sulfate-doped bicelles (and by NOEs within proMMP-7). Format follows that of Movie S2.

SUPPLEMENTAL EXPERIMENTAL PROCEDURES

Preparation of NMR Samples

ProMMP-7(E195A) was expressed and purified as described (Fulcher et al., 2014). Isotopic enrichment was performed in PG media (Studier, 2005). Uniform $^{13}C/^{15}N$ labeling with 70% random deuteration was used for peak assignments and determining the structure of the free state. $^{15}N/^{12}C/^{2}H/ILV\ ^{13}CH_3$ labeling was used for PRE and NOE measurements of complexes with bicelles. The α-keto acids used were from CIL (Cambridge, MA). NMR samples were around 400 μM in 20mM imidazole (pH 6.6), 10 mM $CaCl_2$, 20 μM $ZnCl_2$, 10 mM 2-mercaptoethanol, 0.02% NaN_3, and 10% $^{2}H_2O$. DMPC/DH^{6}PC bicelles were prepared at 1:2 molar ratio (q=0.5) as described (Koppisetti et al., 2014), in order to obtain well-characterized small dimensions and isotropic rotational diffusion (Glover et al., 2001). Their approximate dimensions measured by dynamic light scattering using a DynaPro MSTC. Cholesterol 3-sulfate (CS, Sigma-Aldrich) was dried from methanol:chloroform (1:1 w/w) solution and mixed with bicelle preparations for titrations and typical usage at about six per bicelle. To introduce PREs, DPPC spin-labeled with 5-doxyl, 14-doxyl, or γ-tempo (Avanti Polar Lipids) was added to about two per bicelle.

NMR Spectroscopy

Triple resonance spectra (Bax and Grzesiek, 1993) were used to assign the backbone peaks of proMMP-7. H(CCO)NH (Carlomagno et al., 1996) and HCCH-TOCSY spectra (Peti et al., 2000) were used to assign aliphatic sidechains. (Hb)Cb(CgCd)Hd and (Hb)Cb(CgCd)He spectra (Yamazaki et al., 1993) were used to assign aromatic sidechains. CCP Nmr Analysis 2.4.0 was used for spectral analysis (Vranken et al., 2005). Val and Leu methyl peaks were assigned stereospecifically (Neri et al., 1989). Dihedral angle restraints were calculated by TALOS+ (Shen et al., 2009).

Measurements of apparent translational self-diffusion of bicelle preparations made use of the LED-BPP pulse sequence (Wu et al., 1995). Diffusion decay curves were measured with pulsed field gradients ranging from 3 to 46 G/cm, and were reproduced on both on 600 and 800 MHz Bruker Avance III NMR systems. The diffusion period was 300 ms. The duration of each field gradient pulse within the bipolar pairs was 2 ms.

SUPPLEMENTARY REFERENCES

Bax, A., and Grzesiek, S. (1993). Methodological Advances in Protein NMR. Acc. Chem. Res. *26*, 132-138.

Carlomagno, T., Maurer, M., Sattler, M., Schwendinger, M.G., Glaser, S.J., and Griesinger, C. (1996). PLUSH TACSY: Homonuclear planar TACSY with two-band selective shaped pulses applied to C(alpha),C' transfer and C (beta),C (aromatic) correlations. J. Biomol. NMR *8*, 161-170.

Fulcher, Y.G., Sanganna Gari, R.R., Frey, N.C., Zhang, F., Linhardt, R.J., King, G.M., and Van Doren, S.R. (2014). Heparinoids activate a protease, secreted by mucosa and tumors, via tethering supplemented by allostery. ACS Chem Biol *9*, 957-966.

Glover, K.J., Whiles, J.A., Wu, G., Yu, N.-j., Deems, R., Struppe, J.O., Stark, R.E., Komives, E.A., and Vold, R.R. (2001). Structural Evaluation of Phospholipid Bicelles for Solution-State Studies of Membrane-Associated Biomolecules. Biophys. J. *81*, 2163-2171.

Koppisetti, R.K., Fulcher, Y.G., Jurkevich, A., Prior, S.H., Xu, J., Lenoir, M., Overduin, M., and Van Doren, S.R. (2014). Ambidextrous binding of cell and membrane bilayers by soluble matrix metalloproteinase-12. Nature communications *5*, 5552.

Neri, D., Szyperski, T., Otting, G., Senn, H., and Wuthrich, K. (1989). Stereospecific nuclear magnetic resonance assignments of the methyl groups of valine and leucine in the DNA-binding domain of the 434 repressor by biosynthetically directed fractional 13C labeling. Biochemistry *28*, 7510-7516.

Peti, W., Griesinger, C., and Bermel, W. (2000). Adiabatic TOCSY for C,C and H,H J-transfer. J. Biomol. NMR *18*, 199-205.

Shen, Y., Delaglio, F., Cornilescu, G., and Bax, A. (2009). TALOS+: a hybrid method for predicting protein backbone torsion angles from NMR chemical shifts. J. Biomol. NMR *44*, 213-223.

Studier, F.W. (2005). Protein production by auto-induction in high density shaking cultures. Protein Expr. Purif. *41*, 207-234.

Vranken, W.F., Boucher, W., Stevens, T.J., Fogh, R.H., Pajon, A., Llinas, M., Ulrich, E.L., Markley, J.L., Ionides, J., and Laue, E.D. (2005). The CCPN data model for NMR spectroscopy: Development of a software pipeline. Proteins: Structure, Function, and Bioinformatics *59*, 687-696.

Wu, D., Chen, A., and Johnson, C.S. (1995). An improved diffusion-ordered spectroscopy experiment incorporating bipolar-gradient pulses. Journal of magnetic resonance, Series A *115*, 260-264.

Yamazaki, T., Foreman-Kay, D.J., and Kay, E.L. (1993). Two-Dimensional NMR Experiments for Correlating ^{13}CB and ^{1}H Chemical Shifts of Aromatic Residues in ^{13}C-Labeled Proteins via Scalar Couplings. J. Am. Chem. Soc. *115*, 11054-11055.